ATLAS Deliverable 1.5

Recent Mediterranean Outflow Water and Atlantic Meridional Overturning Circulation correlations

Project acronym:	ATLAS
Grant Agreement:	678760
Deliverable number:	Deliverable 1.5
Deliverable title:	Recent Mediterranean Outflow Water and Atlantic Meridional Overturning Circulation correlations
Work Package:	WP1
Date of completion:	31st October 2018
Authors:	Ángela Mosquera Giménez (IEO), Pedro Vélez-Belchí (IEO)

This project has received funding from the European Union's Horizon 2020 research and innovation programme under grant agreement No 678760 (ATLAS). This output reflects only the author's view and the European Union cannot be held responsible for any use that may be made of the information contained therein.

Table of contents

1. Introduction 3

2. Methodology 4

2.1 The RAPID array 4

2.2 The Argo observing system 5

3. Results 7

3.1 The AMOC 7

3.2 The MOW 9

3.3 Correlation between AMOC and MOW 14

3.4 The MOW at 26°N 15

4. Discussion and conclusions 19

5. Acknowledgments 21

6. References 22

Appendix: Document Information 24

1. Introduction

The ATLAS project works towards improving understanding of the North Atlantic Ocean, in particular, how it is connected, how it functions and how it will respond to future changes. The first step to achieve this goal is the study of the Atlantic Meridional Overturning Circulation (AMOC), since it connects deep-sea ecosystems with the transport of heat, salt, and energy in the whole Atlantic Ocean.

The AMOC is the main contributor to the heat interchange in the North Atlantic (Kanzow *et al.*, 2010). It consists, from a simplified point of view, of an upper transport of warm water to the north and a deep transport of cold water to the equator. Thus, the AMOC carries an important amount of heat, approximately 1.5 PW at 25°N, from the equator to high latitudes (Huisman *et al.*, 2010), helping to regulate the climate, especially in Europe (Bryden *et al.*, 2005). Any slowdown in the AMOC, due to both the natural variability and the anthropogenic climate change, would significantly reduce temperature in the regions around the North Atlantic and even in other parts of the world (Vellinga *et al.,* 2002).

The strength of the AMOC is affected by the input of freshwater in the North Atlantic. Light, fresh water entering in the North Atlantic would produce a reduction in the transport of the AMOC (Willis, 2010), while a supply of salty water, such as the Mediterranean Outflow Water (MOW), would enhance the formation of deep water (Rahmstorf, 1998), strengthening the AMOC (Reid, 1978, 1979; Artale *et al.*, 2002; Cacho *et al.*, 2000), and even stabilizing it (Ivanovic *et al.*, 2014).

The MOW is an intermediate water mass, salty and warm, that is formed when dense Mediterranean water passes through the Strait of Gibraltar and mixes with the North Atlantic Central Water (Daniault *et al.*, 1994). This water mass spreads into the North Atlantic at an average depth of about 1100 m, and its signal can be found as far as Bermuda in the west and Rockall Trough in the north (Bozec *et al.*, 2011). The interchange of water between the Mediterranean and the Atlantic depends on two factors: the geometry of the Strait of Gibraltar, which regulates the total volume of water able to physically pass from one basin to the other, and the density gradient, which contributes to controlling salinity and temperature exchange (Ivanovic *et al.*, 2014).

In this report, in order to determine if the variation of the volume of the MOW is having any effect on the fluctuation of the transport of the AMOC, we will use data from the Argo observing system and RAPID arrays to estimate if there is correlation between the inter-annual to decadal MOW distribution in the eastern Atlantic and the components of the AMOC, in particular with the upper mid-ocean transport (UMO).

2. Methodology

In this work, data from the RAPID array and the Argo observing system will be used.

2.1 The RAPID array

Under the RAPID (2001-2007), RAPID-WATCH (2008-2014) and RAPID-AMOC (2014-2020) programmes, an array of instruments was deployed across the Atlantic, from Morocco to Florida, at 26°N (Figure 1). Those instruments have been measuring temperature, salinity and current velocities from the near surface to the sea floor for approximately 13 years. Those data, combined with observations from the Florida current and satellite measurements of surface winds, have been used to determine the overturning circulation in the North Atlantic.

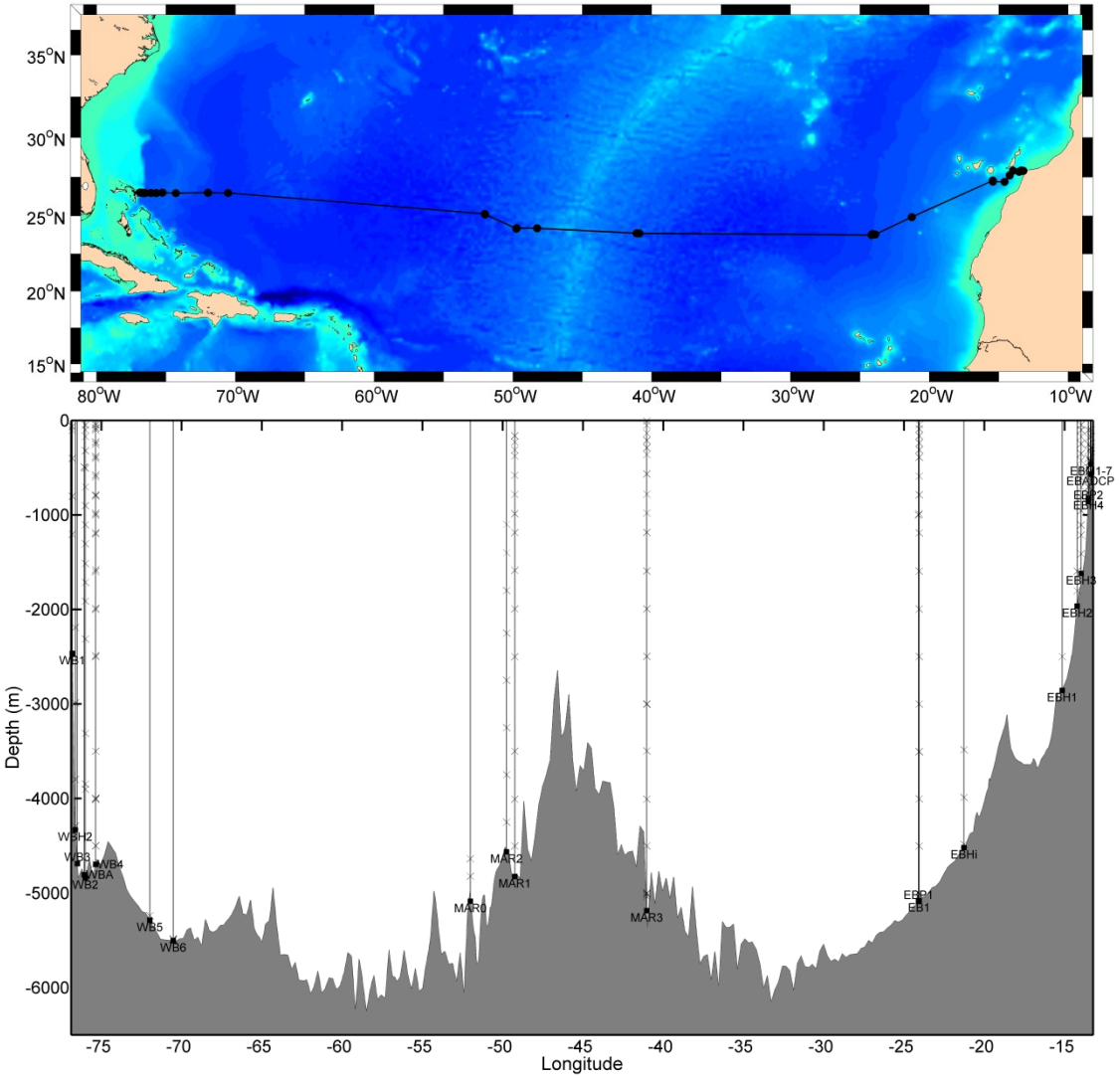

Figure 1. *RAPID array position.*

The products utilized in this work (Smeed *et al.*, 2017) are available to download from the RAPID-AMOC website (http://www.rapid.ac.uk/rapidmoc/) and are summarized in Table 1.

Table 1. RAPID data.

File	MOC Transport Time Series
Description	12-hourly, 10-day low pass filtered transport time series (from April 2004 to February 2017) that includes: • Florida Straits transport. • MOC transport. • Ekman transport. • Upper mid-ocean transport. • Thermocline recirculation (0-800 m). • Intermediate water (800-1100 m). • Upper North Atlantic Deep Water (1100-3000 m). • Lower North Atlantic Deep Water (3000-5000 m). • Antarctic bottom water (> 5000 m).
File	Vertical profiles
Description	12 hourly, 2-day low pass filtered overturning streamfunction (from April 2004 to February 2017).
File	TS gridded data
Description	12-hourly temperature and salinity data merged into five vertical profiles: • Western boundary profiles. • Western boundary mooring WB3. • Western Mid-Atlantic Ridge. • Eastern Mid-Atlantic Ridge. • Eastern boundary profile.

2.2 The Argo observing system

The Argo observing system is an array of around 3800 free-drifting profiling floats distributed globally about each 3° in latitude and longitude (Figure 2). Every 10 days, these floats measure the pressure, temperature and salinity of the first 2000 m of the water column, and once they reach the surface, transmit the recorded information to satellites. These data are publicly available in both near real-time, after an automated quality control, and delayed mode, in annual collections of scientifically quality-controlled data. In addition, the time integrated velocity at depth can also be estimated through the position of the float at the beginning and end of each cycle (Willis and Fu, 2008).

The first floats were deployed in 2000 and the array has been maintained by deploying about 800 new floats every year. In this way, a set of uniformly distributed measurements of temperature, salinity and velocity of the upper ocean have been gathered for about 18 years.

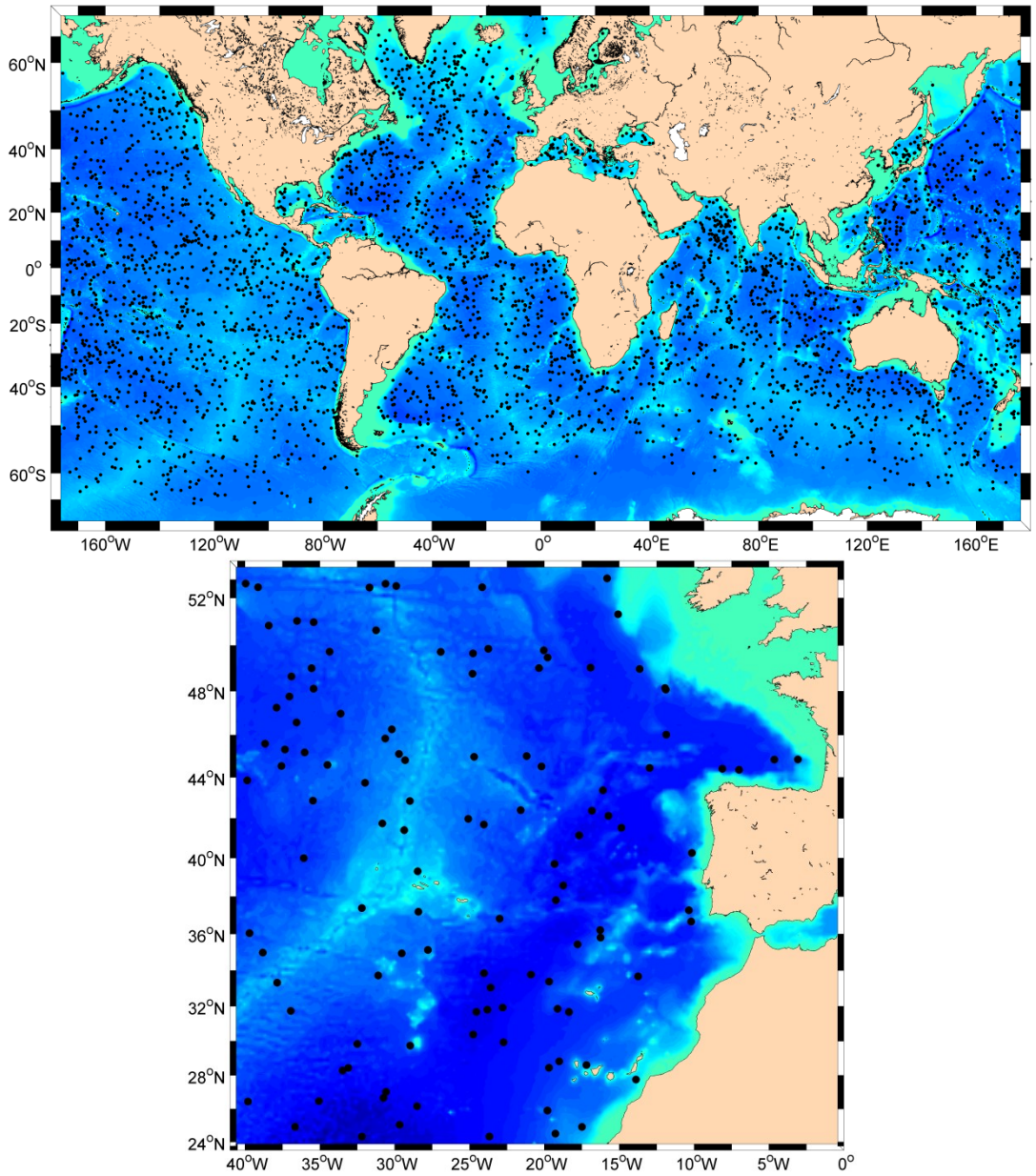

Figure 2. *Positions of Argo floats between 68°N and 68°S in the Northeast Atlantic (from 24th of July to the 14th of August 2018).*

In this work, to estimate the volume of the MOW, we have used the Roemminch-Gilson Argo Climatology (Roemmich and Gilson, 2009) for the period from 2004 to 2016, adding also the monthly extensions from January 2017 to February 2017. This climatology provides values of salinity and temperature, derived from Argo data only, in a regular 1° x 1° grid from surface to about 2000 m.

In addition, the mean field files of temperature and salinity also for the period 2004-2016, with resolution of 1°/6 x 1°/6, were used to analyse the spatial distribution of the main fields of temperature and salinity at the depth of the MOW core.

3. Results

3.1 The AMOC

The MOC, defined as the maximum of the meridional transport integrated from surface to depth, i.e. the maximum of the overturning streamfunction, is found at around 1100 m, as can be observed in Figure 3, where the overturning streamfunction is displayed.

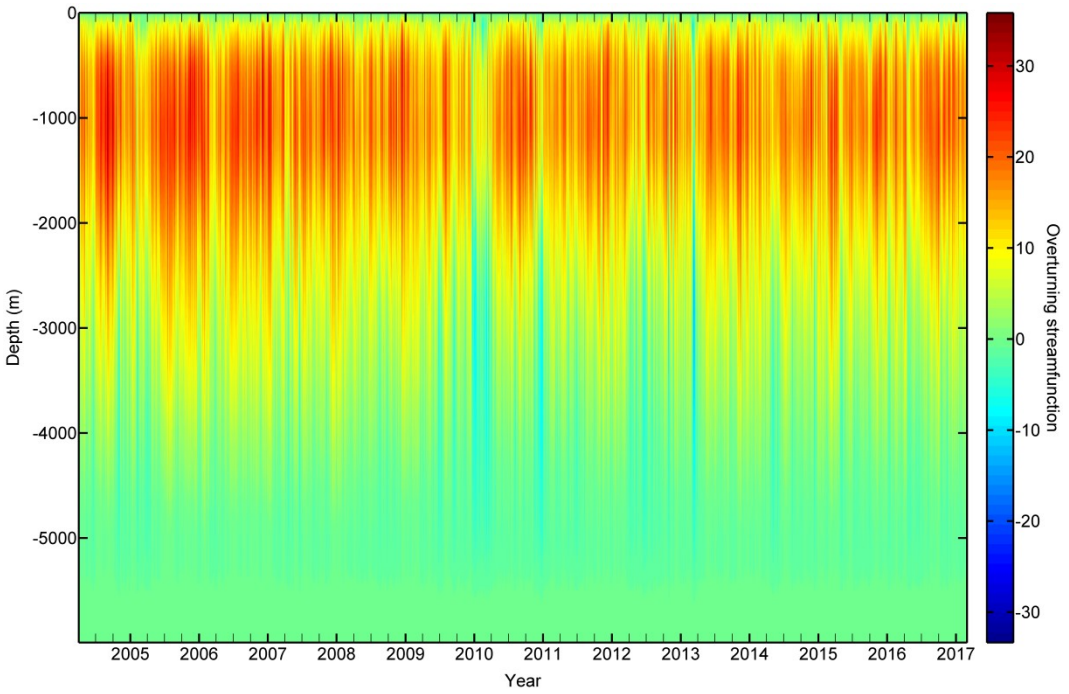

Figure 3. *Overturning streamfunction.*

The time series from RAPID estimates the MOC transport as the sum of three components (Figure 4) (McCarthy *et al.*, 2015): the transport through the Florida Straits, i.e. the volume of water carried by the Gulf Stream; the Ekman transport, result of the interaction between the wind and the ocean surface; and the transport by the upper mid-ocean, derived from the density difference between the water off N America and Africa. For the period from April 2004 to February 2017, these components reach mean values of 31.4±3.2 Sv for the Gulf Stream, 3.7±3.0 Sv for Ekman, and -18.0±3.5 Sv for the upper mid-ocean, which sum a transport of 17.0±4.4 Sv for the MOC.

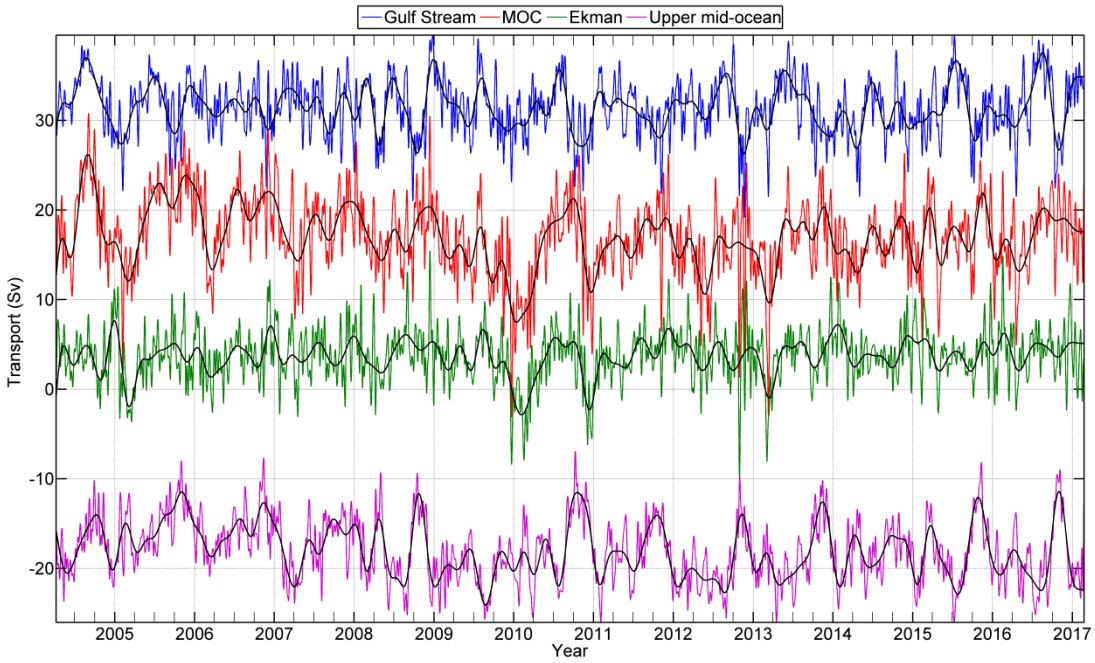

Figure 4. *MOC components. The coloured lines correspond to the 10-day low pass filtered transport data provided by RAPID. The black lines are 90-day filtered data using a 6th-order low pass Butterworth filter.*

The transport for the different layers of the water column is shown in Figure 5. The flow is mainly southwards, except for the intermediate water (800-1100 m) and the Antarctic Bottom Water (>5000 m). The waters between 1100 and 5000 m (corresponding to the Upper and Lower North Atlantic Deep Waters) form the lower limb of the MOC. Their contribution to the flow is of -11.9±2.5 for the Upper NADW and -5.9±2.9 for the Lower NADW. The sum of the transport of those two layers is highly correlated (R^2 of 0.9904) with the transport of the MOC. Therefore, variations in the NADW might affect the MOC.

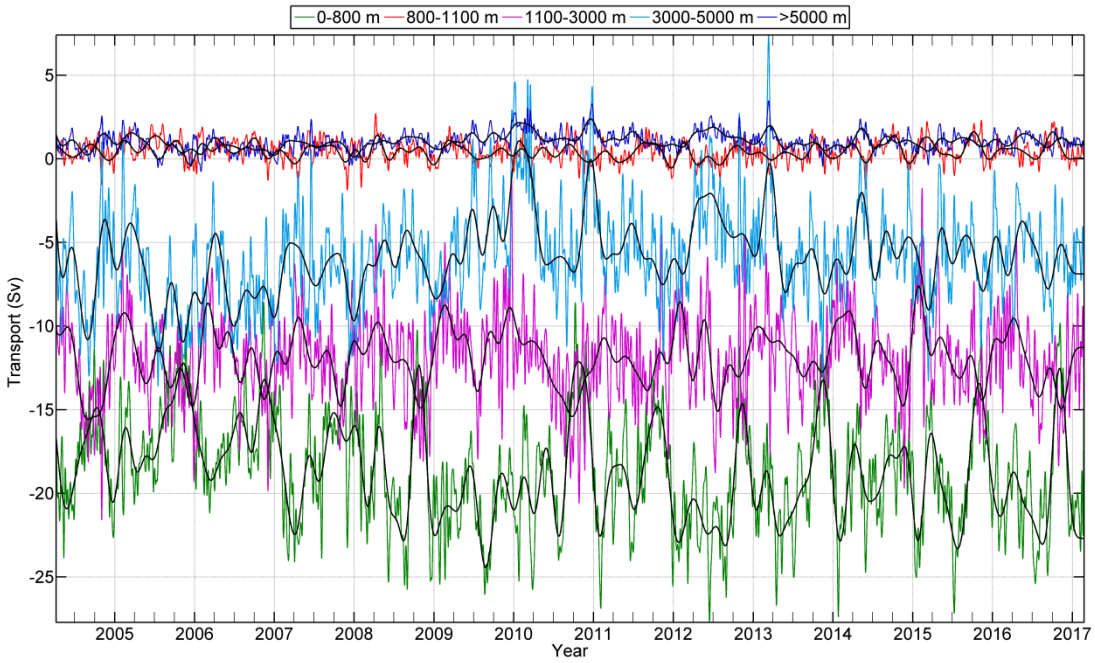

Figure 5. *MOC layers. The coloured lines correspond to the 10-day low pass filtered transport data provided by RAPID. The black lines are 90-day filtered data using a 6th-order low pass Butterworth filter.*

3.2 The MOW

The MOW is characterized by a maximum of salinity at intermediate depths associated with relatively high temperatures (Figure 6).

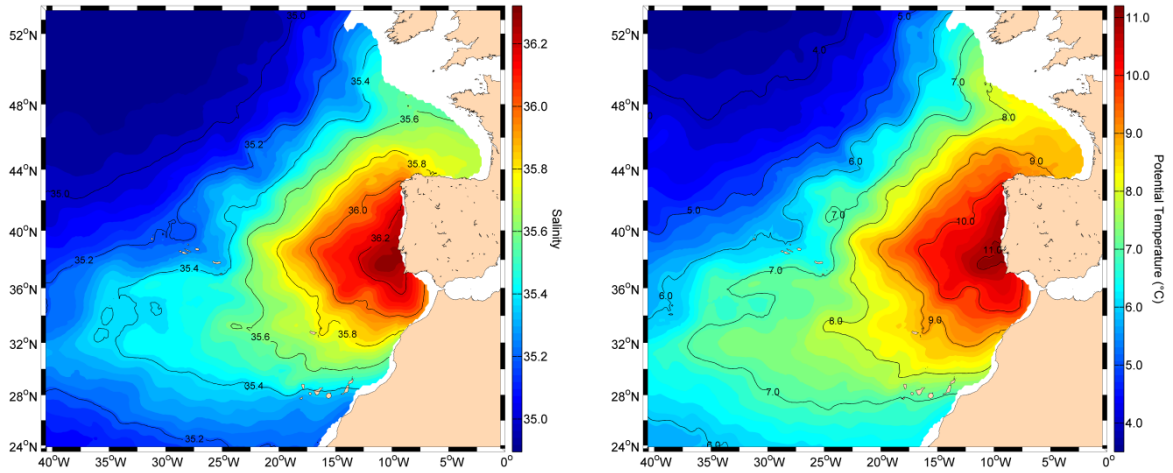

Figure 6. *Mean annual salinity and potential temperature at 1200 db (data from Roemminch-Gilson Argo Climatology for the period 2004-2016).*

Taking into account that the objective of this report is to establish if there is correlation between the amount of MOW and the AMOC, the first step was to estimate the volume of MOW in the Atlantic. The MOW is easily identified in a TS diagram. Therefore we explore different ranges of temperature and salinity to determine the area occupied by the MOW in the most accurate way possible. Once the area was estimated, it was feasible to estimate the volume of MOW. To improve the separation with the other water masses, we also test three different density limits that bound the waters defined as

MOW. In Figure 7 we show a TS diagram of all the profiles in the Roemminch-Gilson Argo Climatology for the geographic area between 53°N 39°W and 25°N 1°W, the three different ranges of temperature and salinity used to determine the MOW volume, and the three isopycnals used to separate the MOW from the other waters masses in the area. The exact values of these ranges can be found in Table 2.

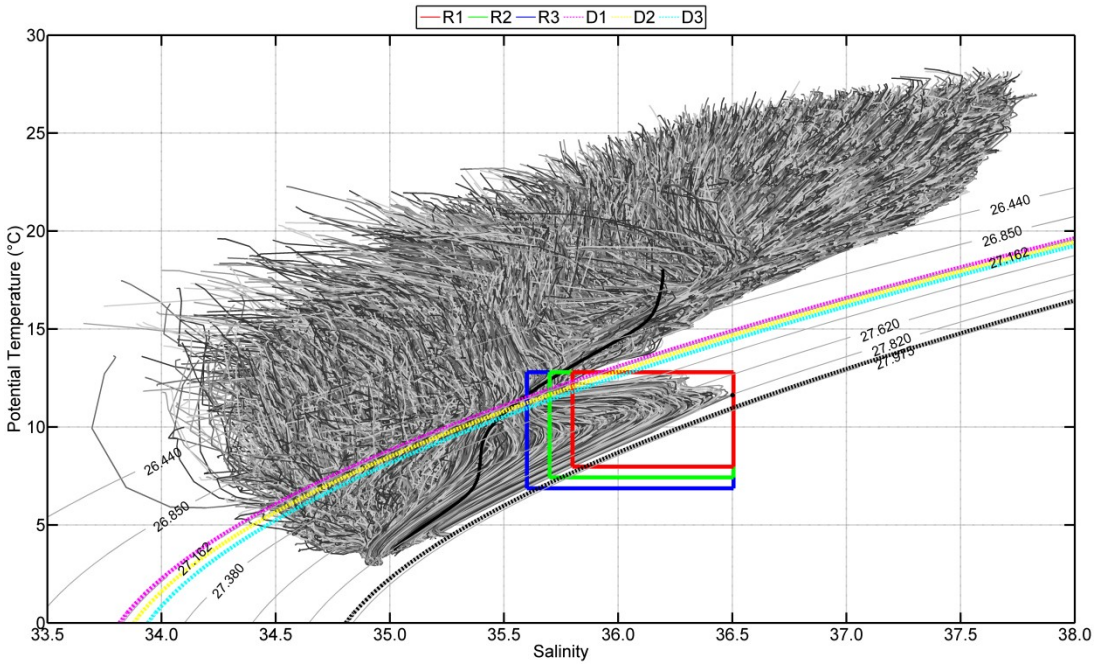

Figure 7. *ϑ/S diagram. The grey lines correspond with the values of temperature and salinity in each point of the grid, while the black line is the mean value. A black dot is located at the maximum of salinity (at 1200 db). The rectangles indicate the ranges of salinity and temperature selected, the black lines are the density lines and the dotted and coloured ones correspond with the density values set as limits. For more information see Table 2.*

Table 2. *Ranges of salinity, potential temperature and density.*

Range TS	Smin	Smax	Tmin	Tmax
R1	35.800	36.505	7.975	12.800
R2	35.700	36.505	7.430	12.800
R3	35.600	36.505	6.870	12.800

Density limits	Minimum	Maximum
D1	27.150	27.950
D2	27.200	27.950
D3	27.250	27.950

At each depth range, we determine the geographical distribution of the Roemminch-Gilson Argo climatology that meet the established conditions of temperature, salinity and density, so that we retrieve the volume occupied by the MOW for a single month. This computation for the period 2004-2017, allowed us to estimate the monthly temporal variation of the MOW volume. A total of 12 different estimations of the volume are represented in Figure 8, where each colour represents the temporal variation at the different ranges of salinity and temperature, while the markers correspond

to the density values used as upper and lower limits and a case where no density boundaries were applied.

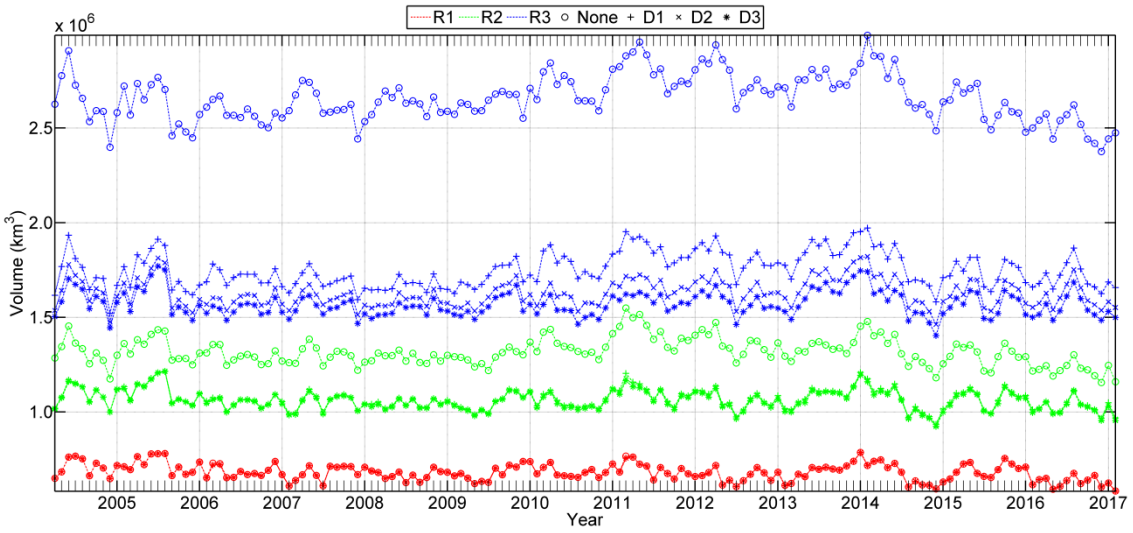

Figure 8. *Time series of the volume of the MOW. The colour of the lines indicates the range of temperature and salinity used and the markers indicate the limits of density being applied.*

Disparities in the different estimations of MOW volume are a consequence of the efficacy of the method in determining the superficial water meeting the defined conditions of salinity and temperature. Thus, the range R3 has the greatest variability, and the volume decreases as the upper density limit increases, since more superficial water is removed from the estimation. The range R2 undergoes a decrease of the total volume after using any density boundary, but there are not noticeable changes between the different density limits. Finally, the range R1 (red line in Figure 8) is more stable than the other two, since it is not practically affected by the density limits. In this manner, the R1 limits are the more robust method of the three to estimate the volume of the MOW, seeing that its results are not sensitive to slight changes in the density boundaries, and the ranges of temperature and salinity defined are enough to delimit the volume occupied by the MOW.

To verify which of the limits used better isolate the MOW, we analysed the mean vertical distribution of the volume of the MOW estimations (Figure 9). In the first 600 m of the water column, there is a big difference between the methods. The temperature and salinity limits set for R3 and R2 are not able to properly discriminate between the superficial water and the water that belongs to the MOW, and it is necessary to add a density limit to improve the estimation. Using D3 as density boundaries, the estimation of the MOW volume at surface is approximately the same for the three ranges of temperature and salinity, and in depth their vertical distribution is also quite similar, reaching the maximum of volume around 1050 db. Thus, a better way of getting a robust estimation of the volume of the MOW is by choosing a depth layer at an intermediate depth. As the MOW is mainly traceable by its high values of salinity, it is more suitable to choose this depth layer based on the mean vertical

distribution of the MOW salinity, instead of the mean vertical distribution of volume. As can be observed in Figure 10, we have selected the depth that coincides with the core of the MOW, as the water there is less mixed and therefore has properties closer to those found for the purest MOW. This core is characterized by a maximum of salinity, and in the area of study it is located approximately at 1200 db.

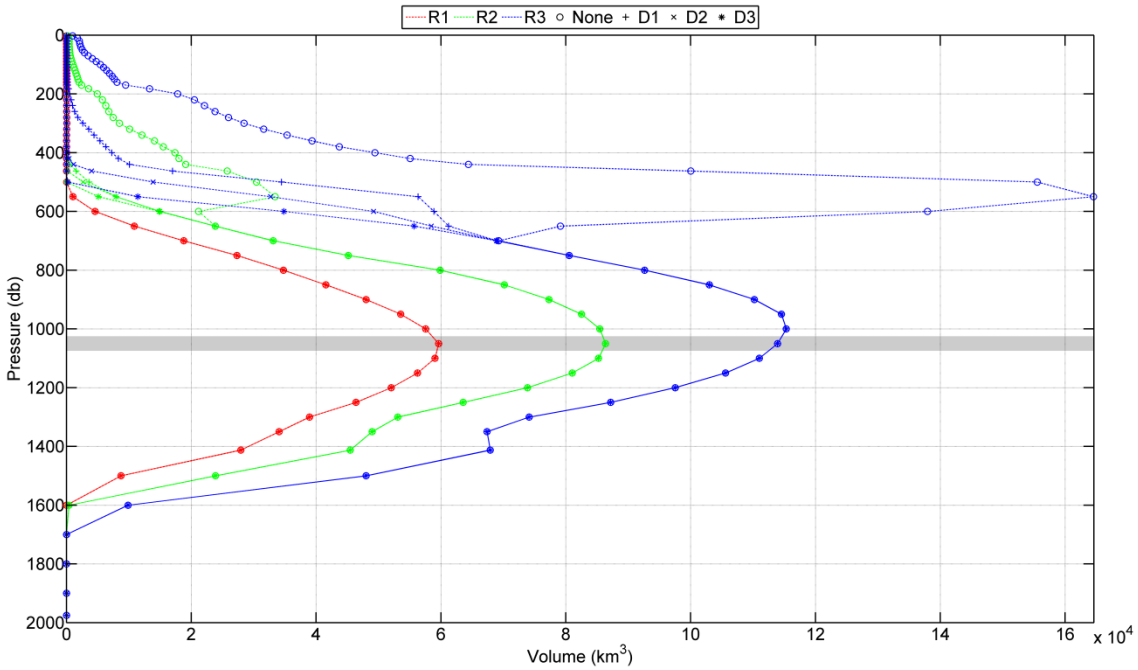

Figure 9. *Mean vertical distribution of MOW volume. The colour of the lines indicates the range of temperature and salinity used and the markers, the limits of density being applied.*

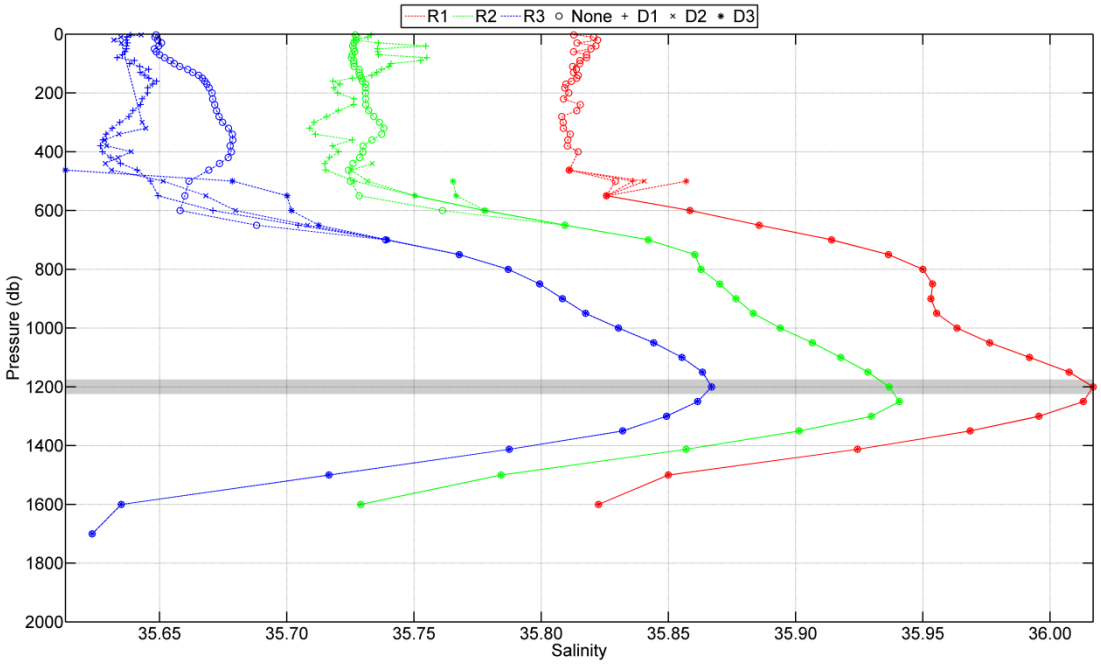

Figure 10. *Mean vertical distribution of salinity in the MOW region, taking into account the volume of each point of the grid. The colour of the lines indicates the range of temperature and salinity used and the markers, the limits of density being applied.*

Determining the area covered by the MOW only at the depth range centred at 1200 db, we can obtain a better estimation of the volume of the MOW at the core for each one of the defined ranges (Figure 11). This time series is, as expected, totally independent of the density limits applied. However, there are still differences among the three ranges of temperature and salinity used, not only in the total volume, but also in the temporal variation. Those discrepancies between the different estimations of the MOW volume are due to the higher amount of water included in the ranges with broader limits, which does not vary accordingly to the water enclosed by the ranges of narrower ones. The wider the range, the greater the possibility of including less pure MOW, which will be affected by other factors that make it vary in a different way, increasing the discrepancies among the estimations.

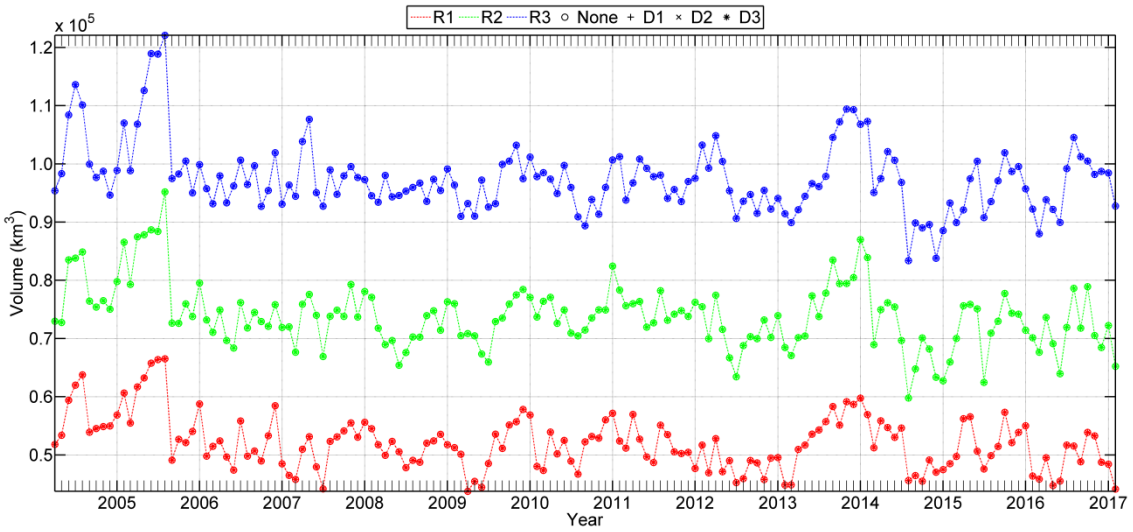

Figure 11. *Time series of the volume of the MOW at 1200 db. The colour of the lines indicates the range of temperature and salinity used and the markers the limits of density being applied.*

In order to verify if the water enclosed by each one of the previous ranges belongs to the MOW, we analysed the horizontal distribution of the volume of the MOW at 1200 db (Figure 12). As we anticipated, as the lower limits of salinity and temperature of the ranges decrease, the area covered by the MOW increases. However, for all the ranges the distribution of the MOW is always coherent with the distribution expected for this water mass. Due to the discrepancies in the estimation of the volume of the MOW and the coherence of the area covered, any range should be rejected in advance, and the three estimations of the volume of the MOW will be equally valid.

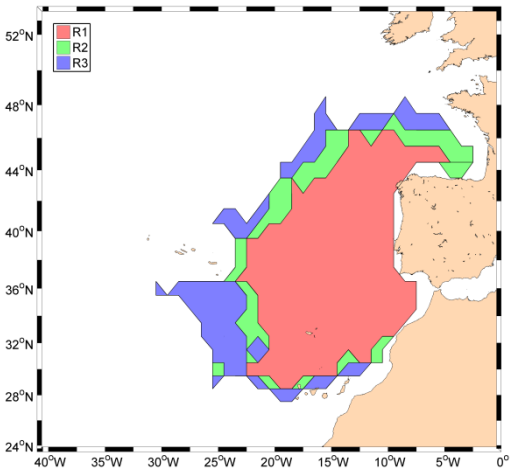

Figure 12. *Horizontal distribution of the volume of the MOW at 1200 db.*

3.3 Correlation between AMOC and MOW

Once the time series of the volume of the MOW for the different ranges was obtained, we proceeded to compare this with the transport time series of the MOC components provided by the RAPID array, in particular with the upper mid-ocean transport, since both the MOW and the upper mid-ocean are driven by density differences. The comparison of this MOC component and the estimation of the volume of the MOW for each of the three ranges showed that overall there is low correlation between the volume of MOW and the upper mid-ocean transport. However, the range R1, the waters with salinity above 35.8, shows high similarity (Figure 13), especially for the period between 2012 and 2017. Thus, the maximums in volume of the MOW are normally near the maximums in the transport of the upper mid-ocean. The coincidence of high values can be found all along the time series, with closer resemblance between the peaks from 2012 to 2017. Besides, both time series show a general trend to decrease, that in some time periods, as for 2011-2012, are quite similar.

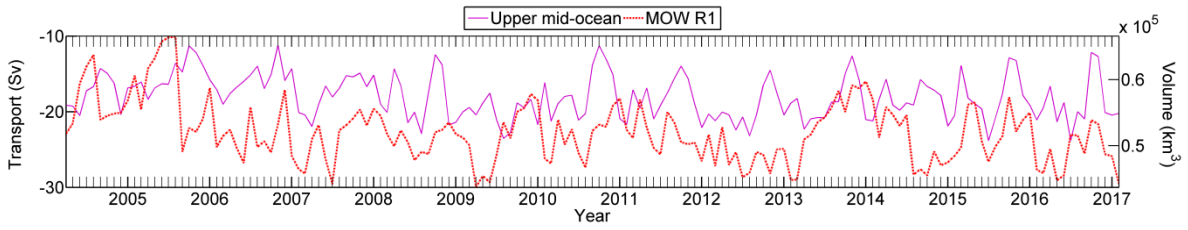

Figure 13. *Upper mid-ocean transport and MOW volume at 1200 db for range R1.*

The comparison of the volume of the MOW and the transport in each layer of the MOC did not show any improvement. The bigger resemblance was found with the circulation in the first 800 m especially when it is compared with the volume estimated using the range R1 (Figure 14). The results were practically identical of those found for the upper mid-ocean, since this MOC component and the transport in this first layer, corresponding to the thermocline recirculation, present a high correlation (R^2 of 0.9886).

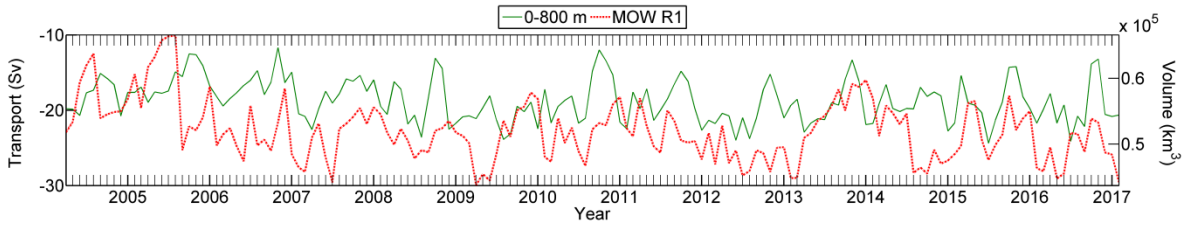

Figure 14. *Transport in the first 800 m of the water column (thermocline recirculation) and MOW volume at 1200 db for range R1.*

In spite of the similarities, the results of applying a linear fit between the MOW volume and the transports corresponding to the upper mid-ocean and the thermocline recirculation give very low correlation coefficients (R^2 of 0.073), improving slightly for the period from 2012 to 2017 (R^2 of 0.088). The noisy character of both time series reduces the value of these correlations.

Therefore, although there is no statistical correlation between the estimation of the volume of the MOW and the MOC components, it is evident that there are similarities between both time series. To further explore the causes of these similarities, we continue the analysis by verifying if a direct contribution of the MOW is affecting the estimations of the MOC at 26°N.

3.4 The MOW at 26°N

The next step is to explore if the amount of MOW that reaches the 26°N fluctuates accordingly with the variation of the total volume estimated for the MOW. Thus, using the temperature and salinity data from the eastern boundary RAPID profile (Figure 15), we could estimate the volume of the MOW reaching the 26°N. Besides, in the same way we did for the Roemmich-Gilson Argo climatology, we defined three new ranges of temperature and salinity with three new boundaries of density (Figure 16 and Table 3) obtaining 12 temporal series of the volume of the MOW in this area.

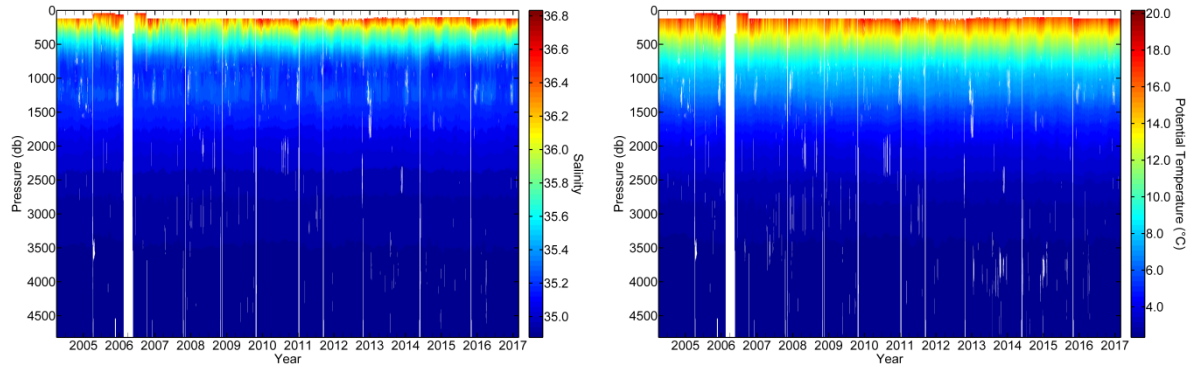

Figure 15. *Eastern boundary profiles of salinity and potential temperature for the period 2004-2017.*

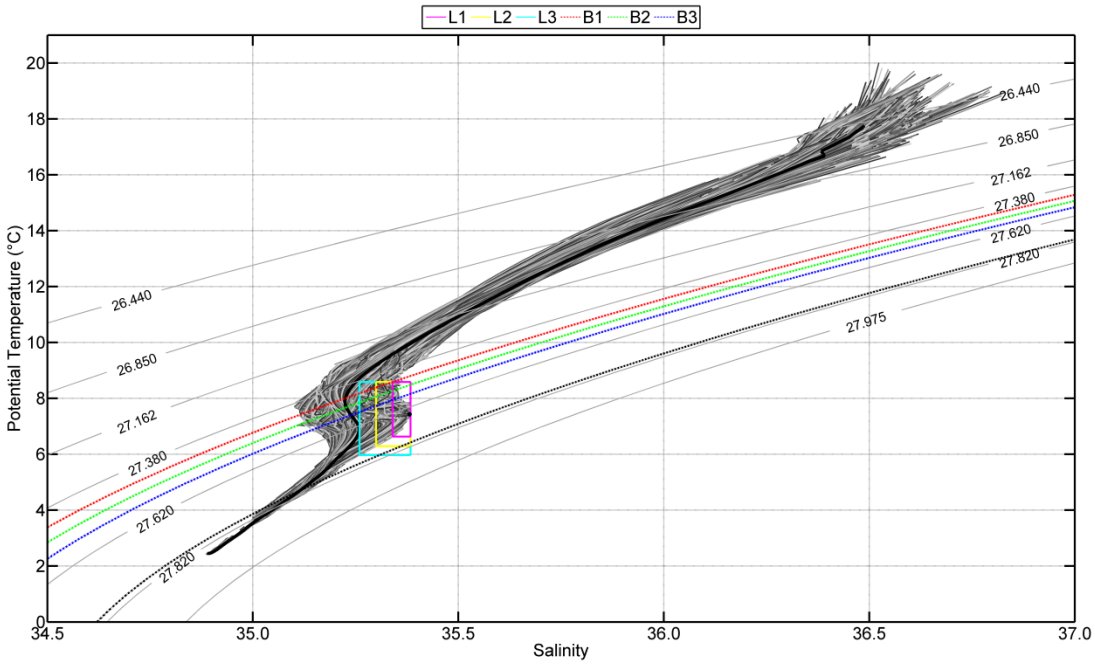

Figure 16. *ϑ/S diagram. The grey lines correspond with the values of temperature and salinity in each point of the grid, while the black line is the mean value. A black dot is located at the maximum of salinity (at 1100 db). The rectangles indicate the ranges of salinity and temperature selected, the black lines are the density lines and the dotted and coloured ones correspond with the density values set as limits. For more information see Table 3.*

Table 3. *Ranges of salinity, potential temperature and density for RAPID data.*

Range TS	Smin	Smax	Tmin	Tmax
L1	35.340	35.384	6.630	8.585
L2	35.300	35.384	6.290	8.585
L3	35.260	35.384	5.970	8.585

Density limits	Minimum	Maximum
B1	27.450	27.800
B2	27.500	27.800
B3	27.550	27.800

The MOW reaching 26°N has lost part of its characteristic temperature and salinity as result of the mixing it has experimented during its southward propagation. For this reason the ranges defined are narrower and fresher than those used for the whole Northeast Atlantic. However, as opposed to the limits defined for that area, at 26°N the ranges with higher salinity show discontinuities in the temporal series, registering the presence of MOW only for few months a year (Figure 17). Those gaps lead to consider lower limits of temperature and salinity, which lead to time series highly dependent of the density boundaries chosen. Thus, to get a robust estimation of the MOW volume, we selected again a depth layer at the MOW core, which, at 26°N, is located at about 1100 db, more than 100 db above the maximum of volume.

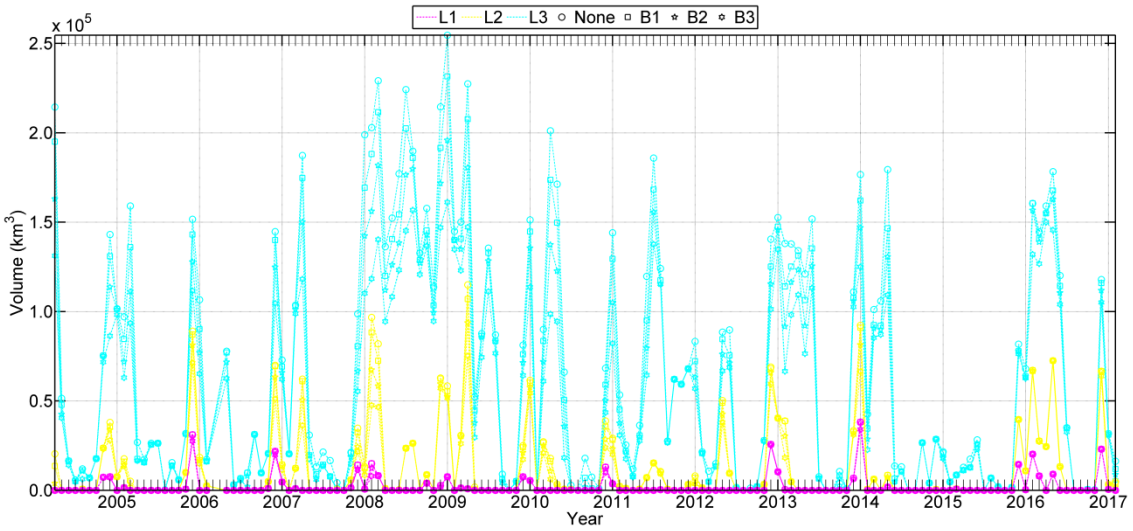

Figure 17. *Time series of the volume of the MOW. The colour of the lines indicates the range of temperature and salinity used, and the markers, the limits of density being applied.*

The results obtained for the estimation of the volume of the MOW at 1100 db are shown in Figure 18. Again, the time series is totally independent of the density, however, there are still gaps where the data did not meet the established ranges for temperature and salinity.

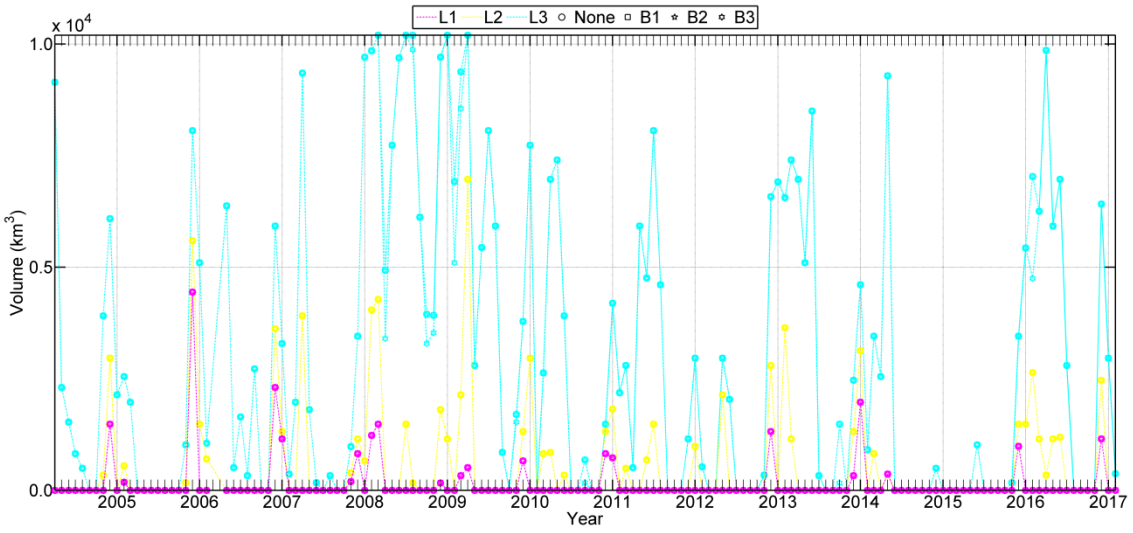

Figure 18. *Time series of the volume of the MOW at 1100 db. The colour of the lines indicates the range of temperature and salinity used, and the markers, the limits of density being applied.*

The time series of MOW volume estimated with RAPID data at 1100 db were compared with those estimated with the Roemmich-Gilson Argo climatology at 1200 db. The highest similarity was found between the volume estimated with the range R3 for the Roemmich-Gilson Argo climatology and the volume estimated with the range L3 for the RAPID data (Figure 19). However, the correlation coefficient was still too low (R^2 of 0.029).

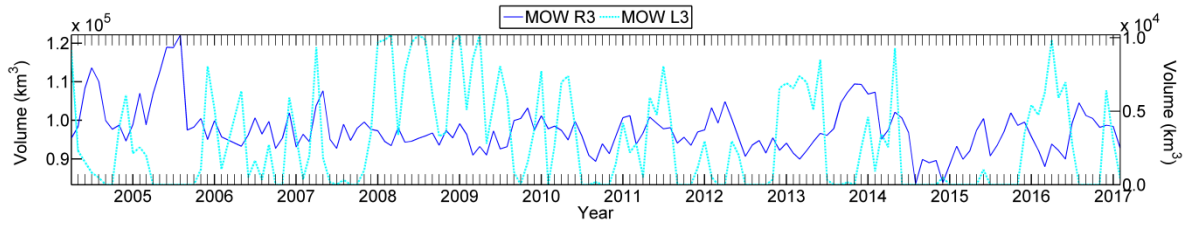

Figure 19. *MOW volume estimated with the Roemmich-Gilson Argo Climatology at 1200 db, range R3, and MOW volume estimated with RAPID data at 1100 db for the range L3.*

Thus, the results of this analysis were even lower than those from the comparison of the volume of the MOW and the upper mid-ocean transport, and no clear resemblance between both time series was identified.

4. Discussion and conclusions

In order to accomplish the objective of this report, and to determine if a **correlation between the MOW distribution in the eastern Atlantic and the AMOC transport** exists, we have developed a method to estimate the volume of the MOW using the Roemmich-Gilson Argo climatology, based on establishing ranges of temperature and salinity. The ranges with lower limits of temperature and salinity did not show a clear differentiation between superficial waters and those belonging to the MOW, and density boundaries should be added to improve the estimation. However, the range with highest salinity did not show those problems. An even more robust estimation was obtained by selecting a depth layer, precisely the depth at the core of the MOW, where the water remains less mixed.

The estimated time series of the volume of the MOW was compared with the MOC components: the Gulf Stream, the Ekman and the upper mid-ocean transports. The best relationship was found between the transport of the upper mid-ocean and the volume estimated with the range of highest salinity at the core, although the correlation coefficient was extremely low. The same relationship was found between the volume of the MOW and the transport in the first 800 m, corresponding to the thermocline recirculation, due to the high similarity with the upper mid-ocean transport. Despite these low correlations, which indicate that the MOW may have no effect on the MOC, the high resemblance of both time series during the period 2012-2017 makes us think that either there is a connection between the MOW and the MOC, or the MOW is directly affecting the estimations of the MOC obtained by the RAPID.

In order to verify if these similarities could be due to the effects of the MOW in the estimations of the MOC computed from the RAPID array data at 26°N, we estimated the volume of the MOW at the core with the data of temperature and salinity provided by RAPID at 26°N, using our method based on ranges. The new time series was compared with the volume estimated with the Roemmich-Gilson Argo climatology. Although, it might seem reasonable to think that when the total volume of the MOW changes, the amount of this water mass reaching 26°N will also change, no evidence was found to support this theory.

Thus, due to this lack of correlation we could conclude that the variation of the volume of the MOW does not seem to affect the strength of the AMOC, neither by modifying their components nor as a direct input at mid-depths. However, given the similarities between the estimated volume of the MOW and the upper mid-ocean transport, the extremely low correlation values could be mostly a consequence of a delayed response with a variable lag or to the noisy character of the time series.

The hypothesis that we proposed to explain the similarity between the estimations of the MOW and the AMOC, especially in the period 2012-2017, is that the changes that occur in all the Atlantic, observed by the RAPID array, also affect the exchange between the Atlantic and the Mediterranean, and therefore to the volume of MOW in the Atlantic.

5. Acknowledgments

Data from the RAPID MOC monitoring project are funded by the Natural Environment Research Council and are freely available from http://www.rapid.ac.uk/rapidmoc/ (doi: 10.5285/5acfd143-1104-7b58-e053-6c86abc0d94b). The Roemmich-Gilson Argo Climatology is freely available from http://sio-argo.ucsd.edu/.

6. References

Artale, V., Calmanti, S., and Sutera, A., 2002. Thermohaline circulation sensitivity to intermediate-level anomalies. *Tellus*, 54A, 159-174, doi: 10.1034/j.1600-0870.2002.01284.x.

Bozec, A., Lozier, M. S., Chassignet, E. P., and Halliwell, R., 2011. On the variability of the Mediterranean Outflow Water in the North Atlantic from 1948 to 2006. *Journal of Geophysical Research*, 116, C09033, doi:10.1029/2011JC007191.

Bryden, H. L., Longworth, H. R., and Cunningham, S. A., 2005. Slowing of the Atlantic meridional overturning circulation at 25°N. *Nature*, 438, 655-657, doi: 10.1038/nature04385.

Cacho, I., Grimalt, J. O., Sierro, F. J., Shckleton, N., and Canals, M., 2000. Evidence for enhanced Mediterranean thermohaline circulation during rapid climatic coolings. *Earth and Planetary Science Letters*, 183, 417-429, doi: 10.1016/S0012-821X(00)00296-X.

Daniault, N., Mazé, J. P., and Arhan, M., 1994. Circulation and mixing of Mediterranean Water west of the Iberian Peninsula. *Deep-Sea Research I*, 41(11-12), 1685-1714, doi: 10.1016/0967-0637(94)90068-X.

Huisman, S. E., den Toom, M., and Dijkstra, H. A., 2010. An indicator of the multiple equilibria regime of the Atlantic Meridional Overturning Circulation. *Journal of Physical Oceanography*, 40, 551-567, doi: 10.1175/2009JPO4215.1.

Ivanovic, R. F., Valdes, P. J., Gregoire, L., Flecker, R., and Gutjahr, M., 2014. Sensitivity of modern climate to the presence, strength and salinity of Mediterranean-Atlantic exchange in a global general circulation model. *Climate Dynamics*, 42(3-4), 859-877, doi: 10.1007/s00382-013-1680-5.

Kanzow, T., Cunningham, S. A., Johns, W. E., Hirschi, J. J.-M., Marotzke, J., Baringer, M. O., Meinen, C. S., Chidichimo, M. P., Atkinson, C., Beal, L. M., Bryden, H. L., and Collins, J., 2010. Seasonal variability of the Atlantic Meridional Overturning Circulation at 26.5°N. *Journal of Climate*, 23, 5678-5698, doi: 10.1175/2010JCLI3389.1.

McCarthy, G. D., Smeed, D. A., Johns, W. E., Frajka-Williams, E., Moat, B. I., Rayner, D., Baringer, M. O., Meinen, C. S., Collins, J., and Bryden, H. L., 2015. Measuring the Atlantic Meridional Overturning Circulation at 26°N. Progress in Oceanography, 130, 91-111, doi: 10.1016/j.pocean.2014.10.006.

Rahmstorf, S., 1998. Influences of Mediterranean outflow on climate. *Eos,* 79(24), 281-282, doi: 10.1029/98EO00208.

Reid, J. L., 1978, On the middepth circulation and salinity field in the North Atlantic Ocean. *Journal of Geophysical Research*, 83(C10), 5063-5067, doi: 10.1029/JC083iC10p05063.

Reid, J. L., 1979. On the contribution of the Mediterranean Sea outflow to the Norwegian-Greenland Sea. *Deep-Sea Research*, 26A, 1199-1223, doi: 10.1016/0198-0149(79)90064-5.

Roemmich, D., and Gilson, J., 2009. The 2004-2008 mean and annual cycle of temperature, salinity, and steric height in the global ocean from the Argo Program. *Progress in Oceanography*, 82, 81-100, doi: 10.1016/j.pocean.2009.03.004.

Smeed, D., McCarthy, G., Rayner, D., Moat, B. I., Johns, W. E., Baringer, M. O., and Meinen, C. S., 2017. Atlantic Meridional Overturning Circulation observed by the RAPID-MOCHA-WBTS (RAPID-Meridional Overturning Circulation and Heatflux Array-Western Boundary Time Series) array at 26N from 2004 to2017. British Oceanographic Data Centre - Natural Environment Research Council, UK, doi: 10.5285/5acfd143-1104-7b58-e053-6c86abc0d94b.

Vellinga, M., Wood, R. A., and Gregory, J. M., 2002. Processes governing the recovery of a perturbed thermohaline circulation in HadCM3. *Journal of Climate*, 15, 764-780, doi: 10.1175/1520-0442(2002)015<0764:PGTROA>2.0.CO;2.

Willis, J. K., 2010. Can in situ floats and satellite altimeters detect long-term changes in Atlantic Ocean overturning? *Geophysical Research Letters*, 37, L06602, doi: 10.1029/2010GL042372.

Willis, J. K., and Fu, L.-L., 2008. Combining altimeter and subsurface float data to estimate the time-averaged circulation in the upper ocean. *Journal of Geophysical Research*, 113, C12017, doi: 10.1029/2007JC004690.

Appendix: Document Information

EU Project N°	678760	**Acronym**	ATLAS
Full Title	A trans-Atlantic assessment and deep-water ecosystem-based spatial management plan for Europe		
Project website	www.eu-atlas.org		

Deliverable	**N°**	1.5	**Title**	Recent Mediterranean Outflow Water and Atlantic Meridional Overturning Circulation correlations
Work Package	**N°**	1	**Title**	Ocean Dynamics Driving Ecosystem Response

Date of delivery	**Contractual**
Dissemination level	Confidential

Authors (Partner)	**IEO**			
Responsible Authors	**Name**	Ángela Mosquera Giménez	**Email**	angela.mosquera@ieo.es
		Pedro Vélez-Belchí		pedro.velez@ieo.es

Version log			
Issue Date	**Revision N°**	**Author**	**Change**